Electronic Supplementary Information (ESI) for

Leaping across the visible range: near-infrared-to-violet photon upconversion employing a silyl-substituted anthracene

Rena Haruki,[a] Yoichi Sasaki,[a] Kouta Masutani,[a] Nobuhiro Yanai,*[a,b] and Nobuo Kimizuka* [a]

[a]Department of Chemistry and Biochemistry, Graduate School of Engineering, Center for Molecular Systems (CMS), Kyushu University, 744 Moto-oka, Nishi-ku, Fukuoka 819-0395, Japan.

[b]PRESTO, JST, Honcho 4-1-8, Kawaguchi, Saitama 332-0012, Japan.

E-mail: yanai@mail.cstm.kyushu-u.ac.jp, n-kimi@mail.cstm.kyushu-u.ac.jp

Materials.

All reagents and solvents for synthesis were used as received without further purifications otherwise noted. Pt(II) octaethylporphyrin (PtOEP) was purchased from Aldrich, indocyanine green was purchased from Wako, and they were used as received. 9,10-diphenylanthracene (DPA) was purchased from Tokyo Chemical Industry (TCI) and purified by sublimation at 200°C and ca. 100 Pa. Anthracene was purchased from Aldrich and purified by sublimation at 180°C and ca. 100 Pa. For TTA-UC measurements, the solutions were prepared in an Ar-filled glove box (oxygen concentration < 0.1 ppm) using dehydrated tetrahydrofuran (THF) purchased from Wako.

Characterizations.

^{1}H-NMR (400 MHz) and ^{13}C-NMR (101 MHz) spectra were measured on a JNM-ECZ 400S using TMS as the internal standard. Mass spectroscopy analysis was conducted on a Bruker Autoflex III. Elemental analysis was carried out by using Yanaco CHN Corder MT-5 at the Elemental Analysis Center, Kyushu University. UV-vis absorption spectra were recorded on a JASCO V-770 spectrophotometer. Fluorescence spectra were measured by using a PerkinElmer LS 55 fluorescence spectrometer. The samples were excited at an incidence angle of 45° to the quarts cell surface, and the fluorescence was detected along the normal. The absolute fluorescence quantum yield was measured in an integrating sphere using a HAMAMATSU multichannel analyzer C10027-01.

For TTA-UC emission spectra, a 724 nm diode lasers (40 mW, RGB Photonics) was used as the excitation source. The laser power controlled by combining a software (Ltune) and a variable neutral density filter and measured using a PD300-UV photodiode sensor (OPHIR Photonics). The laser beam was focused on a sample using a lens. The diameters of the laser beam ($1/e^2$) were measured at the sample position using a CCD beam profiler SP620 (OPHIR Photonics). The typical area of laser irradiation spot estimated from the diameter was 1.0×10^{-4} cm^2. The emitted light was removed using a 610 nm short-pass filter, and the emitted light was again focused by an achromatic lens to an optical fiber connected to a multichannel detector MCPD-9800 (Otsuka Electronics).

Time-resolved photoluminescence lifetime measurements were carried out by using a time-correlated single-photon counting lifetime spectroscopy system, HAMAMATSU Quantaurus-Tau C11567-01. The TTA-UC quantum yield of a solid sample was determined by an absolute quantum yield measurement system C13534-01 (Hamamatsu Photonics). The sample was held in an integrating sphere and excited by the laser source (724 nm, 40 mW, RGB Photonics). The scattered excitation light was removed using a 700 nm short-pass filter and emitted light as monitored with a multichannel detector. The spectrometer was calibrated, including the integration sphere and short-pass filter by Hamamatsu Photonics.

Determination of relative TTA-UC quantum efficiency.

Relative upconversion luminescence quantum efficiency (Φ_{UC}') in deaerated THF was determined relative to a standard according to the following equation,[1]

$$\Phi_{UC}' = 2\Phi_{std}\left(\frac{1-10^{-A_{std}}}{1-10^{-A_{UC}}}\right)\left(\frac{I_{UC}}{I_{std}}\right)\left(\frac{P_{std}}{P_{UC}}\right)\left(\frac{\eta_{UC}}{\eta_{std}}\right)^2$$

where Φ, A, I, P and η represent the quantum yield, absorbance at the excitation wavelength, integrated photoluminescence spectral profile, excitation intensity, and the refractive index of the medium, respectively. The subscripts UC and std denote the parameters of the upconversion and standard systems. Note that the theoretical maximum of Φ_{UC}' is standardized to be 1 (100%). For the standard, indocyanine green (5 μM) in DMF with an absolute fluorescence quantum yield of 17.3% was used. The refractive indexes of THF and DMF are 1.407 and 1.430, respectively, at 298 K.[2]

Determination of TET efficiency.

TET efficiency (Φ_{TET}) from donor to acceptor was determined by comparing the phosphorescence intensity of donor in the absence and presence of acceptor based on the following equation,

$$\Phi_{TET} = 1 - \frac{\Phi_P}{\Phi_{P,0}} = 1 - \left(\frac{I_P}{I_{P,0}}\right)\left(\frac{P_{P,0}}{P_P}\right)$$

where $\Phi_{P,0}$ and Φ_P represent the phosphorescence quantum yield of $Os(tpy)_2^{2+}$ (20 μM) in deaerated THF in the absence and presence of acceptor, I and P represent the integrated phosphorescence spectral profile and excitation intensity at 532 nm. Note that the same mother solution of $Os(tpy)_2^{2+}$ was added to different amounts of acceptor (i-$Pr_2SiH)_2An$ to prepare the mixed solutions. Thus the absorbance at the excitation intensity can be assumed to be nearly identical for these solutions.

DFT calculations

Density functional theory (DFT) and time-dependent DFT (TD-DFT) calculations were conducted with the B3LYP exchange-correlation functional as implemented in the Gaussian 09 software.[3] The optimized ground-state structures of (i-$Pr_2SiH)_2An$, anthracene, and DPA were obtained with 6-311G(d,p) basis set. Then, TD-DFT was employed with 6-311++G(d,p) basis set to study the excited-state properties.

Synthetic procedures.

Scheme S1. Synthetic route of $(i\text{-}Pr_2SiH)_2An$ [4]

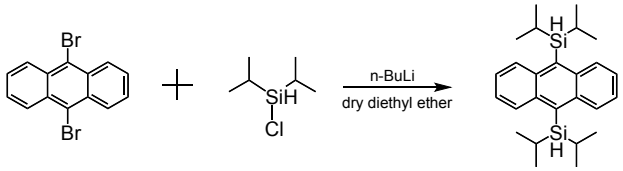

To a suspension of 9,10-dibromoanthracene (1.3 g, 3.87 mmol) in 30 mL of dry diethyl ether, a solution of *n*-butyllithium in hexane (2.6 M, 3.72 mL, 9.67 mmol) was added dropwise at 0°C under N_2 atmosphere. The mixture was allowed to warm gradually to room temperature and stirred for 30 minutes. Chlorodiisopropylsilane (1.99 mL, 11.6 mmol) was added dropwise to the solution, and the mixture was stirred at room temperature for 20 hours. After adding 10 mL of H_2O to the mixture slowly, 50 mL of H_2O was added again and the mixture was washed with $CHCl_3$ (3×50 mL). The organic phase was dried over sodium sulfate and evaporated under reduced pressure. The resulting product was purified by column chromatography (SiO_2, solvent: hexane), gel permeation chromatography (solvent: $CHCl_3$), and reprecipitation in MeOH to give a pale yellow solid. Yield 440 mg (28%). ^{1}H-NMR (400 MHz, $CDCl_3$, TMS): δ 8.69-8.43 (m, 4H), 7.58-7.38 (m, 4H), 4.93-4.78 (t, 2H), 1.78-1.57 (m, 4H), 1.38-1.20 (d, 12H), 0.94-0.77 (d, 12H). ^{13}C-NMR (101 MHz, $CDCl_3$, TMS): δ 136.96, 135.77, 129.76, 124.34, 20.53, 19.83, 13.84. MS (MALDI): m/z = 405.5 (M^+). Elemental analysis: calculated for $C_{26}H_{38}Si_2$: C 76.77 H 9.42, found C 76.68 H 9.35.

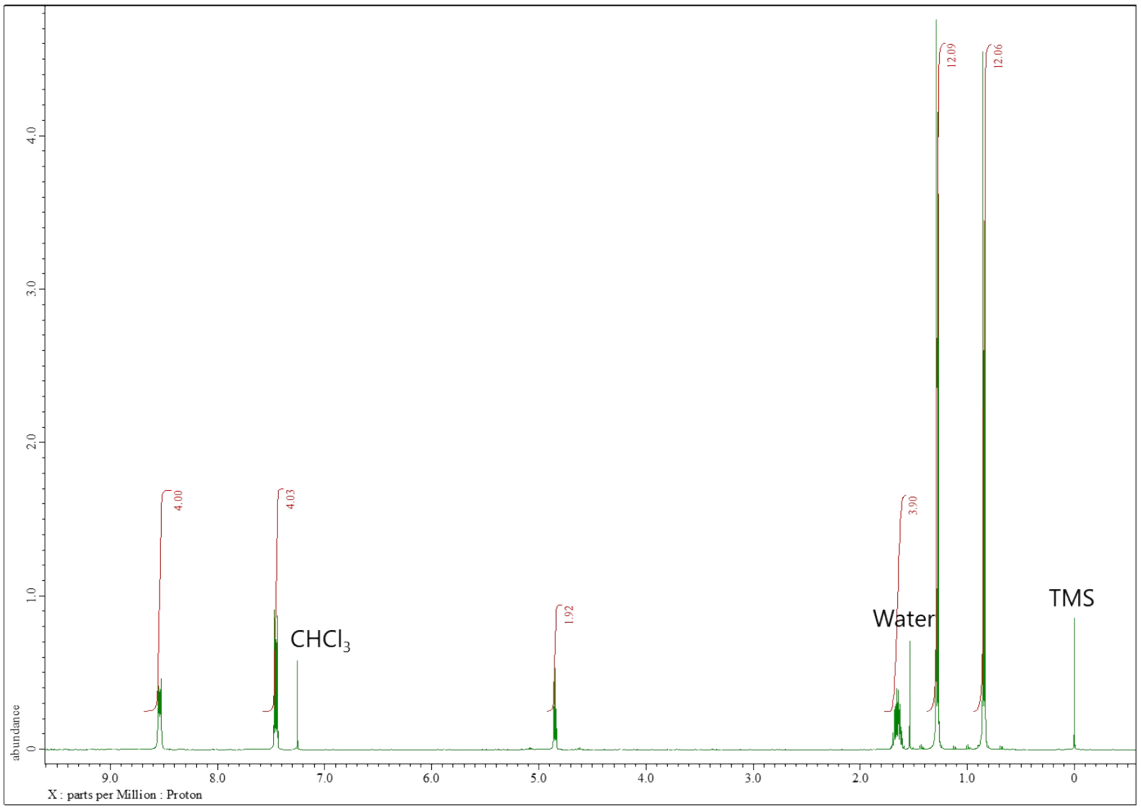

^{1}H-NMR spectra (400 MHz, $CDCl_3$, TMS) of $(i\text{-}Pr_2SiH)_2An$

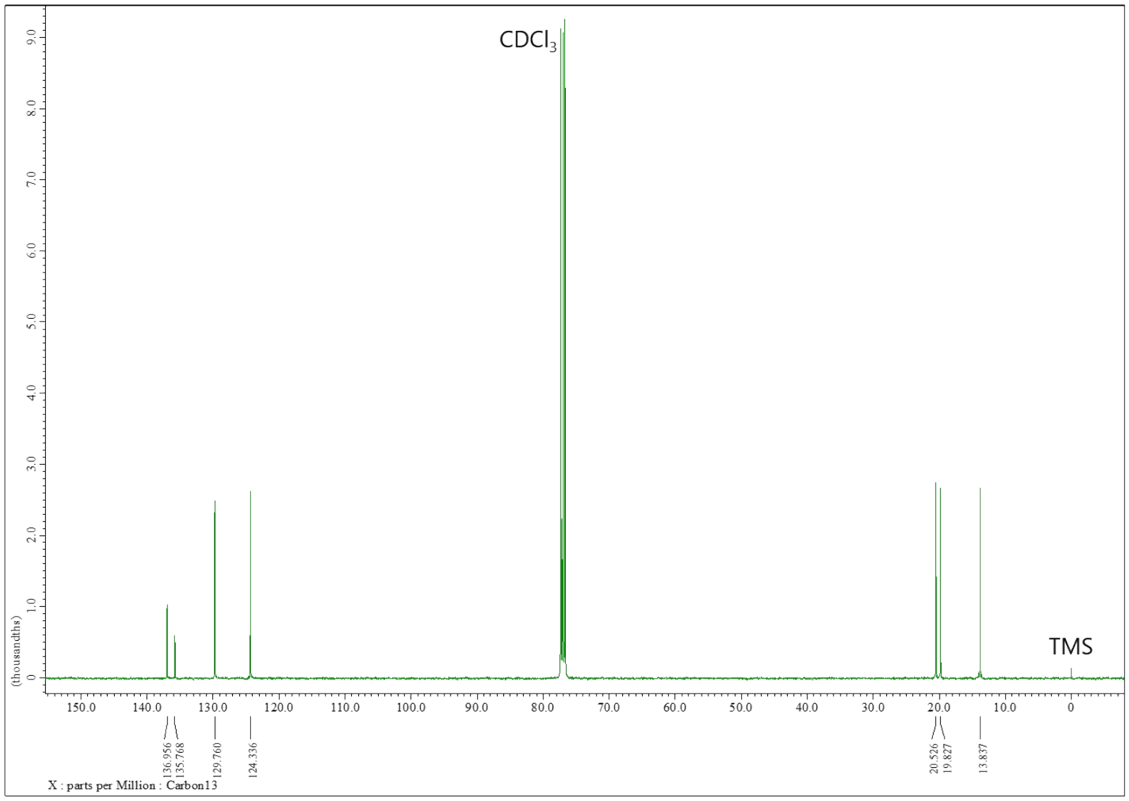

^{13}C-NMR spectra (101 MHz, $CDCl_3$, TMS) of (i-$Pr_2SiH)_2$An

Scheme S2. Synthetic route of $Os(tpy)_2(TFSI)_2$ [5]

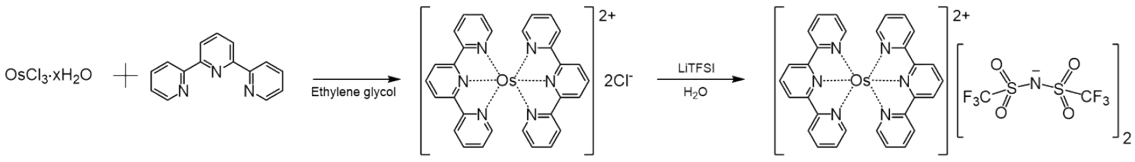

Osmium(III) chloride hydrate (50 mg, ca. 0.17 mmol) and 2,2':6',2''-terpyridine (79 mg, 0.34 mmol) were refluxed in 2.5 mL of ethylene glycol for 2 hours at 230°C using a microwave (Biotage Initiator 2.5) under continuous stirring. After cooling to room temperature, the dark brown solution was added to 20 mL of the aqueous solution of lithium bis(trifluoromethanesulfonyl)imide (200 mg, 70 mmol) and the mixture was stirred for 1 hour. The precipitates were filtrated and washed by ionized water and toluene. The solid was dissolved into acetonitrile and condensed after filtration. The product was purified by reprecipitation in toluene to give a brown solid. Yield 120 mg (59%). ^{1}H-NMR (400 MHz, DMSO-D6, TMS): δ 9.18-9.02 (d, 4H), 8.88-8.73 (d, 4H), 8.12-7.99 (t, 2H), 7.96-7.81 (t, 4H), 7.38-7.25 (d, 4H), 7.25-7.12 (t, 4H). ^{13}C-NMR (101 MHz, DMSO-D6, TMS): δ 159.31, 154.24, 151.92, 137.70, 134.87, 127.84, 124.54, 122.64, 120.95, 117.72. MS (MALDI): m/z = 656.7 ($[Os(tpy)_2-H]^+$) 935.9 ($[Os(tpy)_2+TFSI]^+$). Elemental

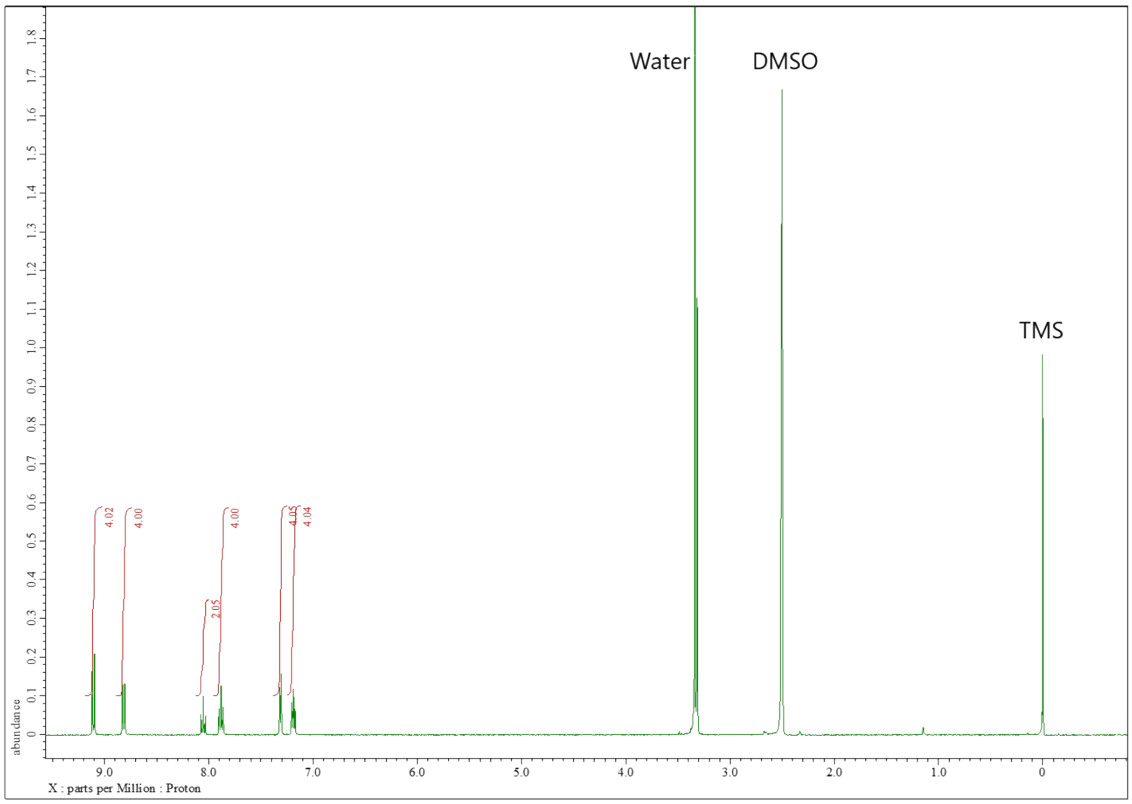

analysis: calculated for $C_{34}H_{22}F_{12}N_8O_8OsS_4$: C 33.55 H 1.82 N 9.21, found C 33.55 H 1.88 N 9.16.

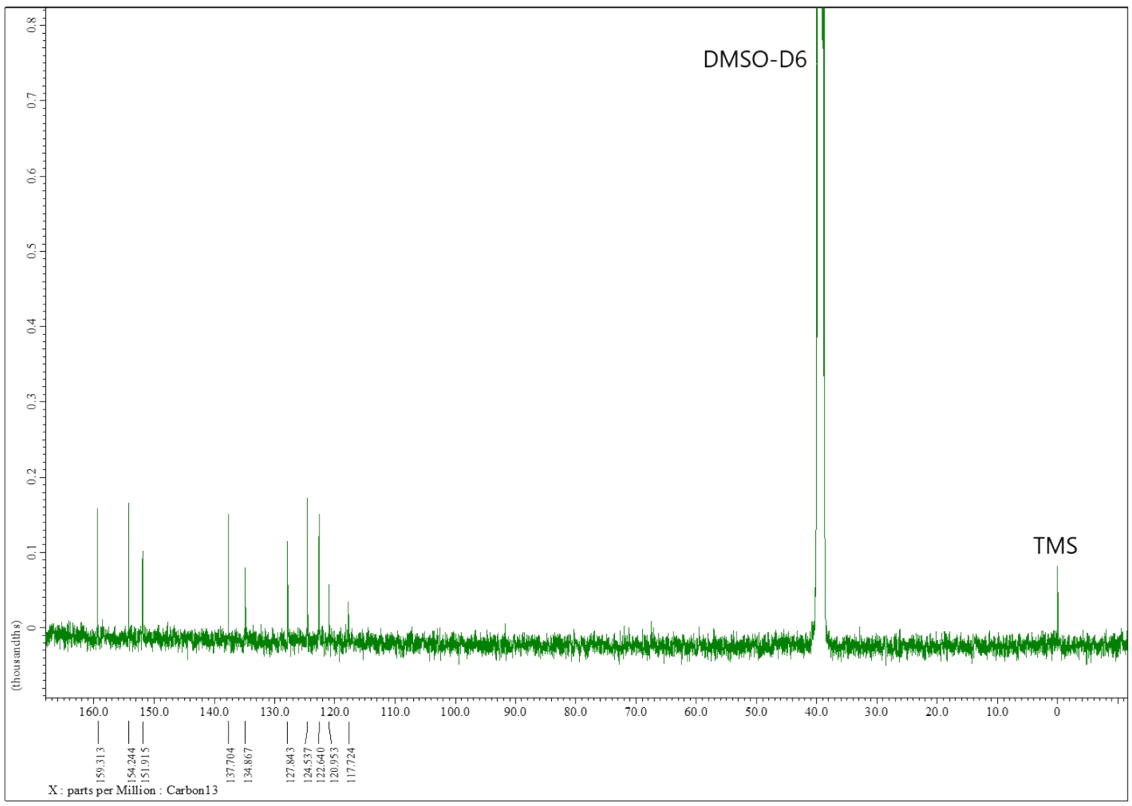

^{1}H-NMR spectra (400 MHz, DMSO-D6, TMS) of $Os(tpy)_2(TFSI)_2$

^{13}C-NMR spectra (101 MHz, DMSO-D6, TMS) of $Os(tpy)_2(TFSI)_2$

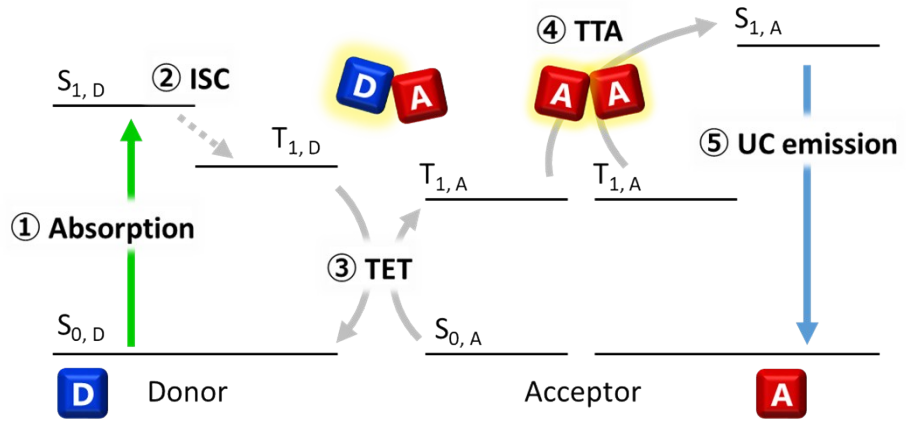

Figure S1. Schematic illustration for the typical TTA-UC mechanism of donor/acceptor pair (S: singlet state, T: triplet state). Green and blue arrows indicate that the absorption and UC emission processes, respectively. In this conventional mechanism, a donor triplet state is generated via the intersystem crossing (ISC) after absorption. TET: triplet energy transfer, TTA: triplet-triplet annihilation.

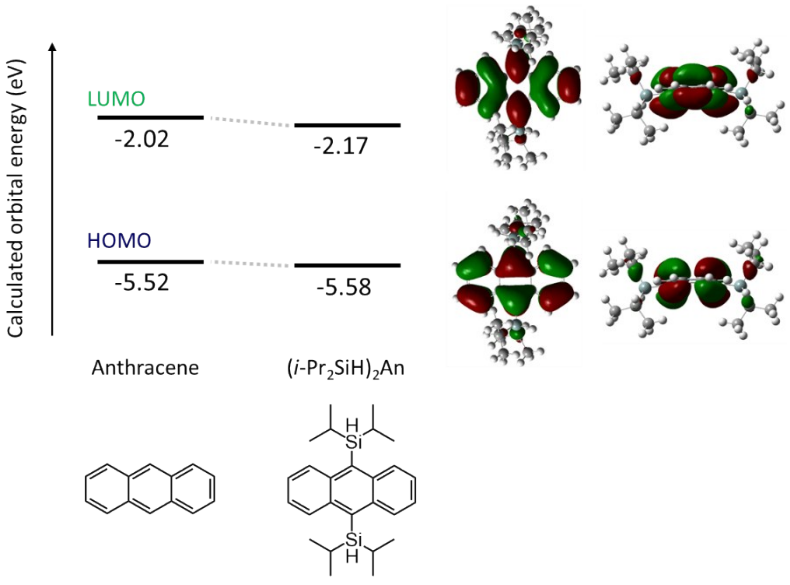

Figure S2. Calculated orbital energy levels in vacuum of anthracene and (*i*-$Pr_2SiH)_2$An and the molecular orbitals of (*i*-$Pr_2SiH)_2$An visualized by Gauss View 5.0.[6] (isovalue = 0.02). The energy levels were calculated at TD-B3LYP/6-311++G (d,p)//B3LYP/6-311G(d,p) in the Gaussian 09 software.[3]

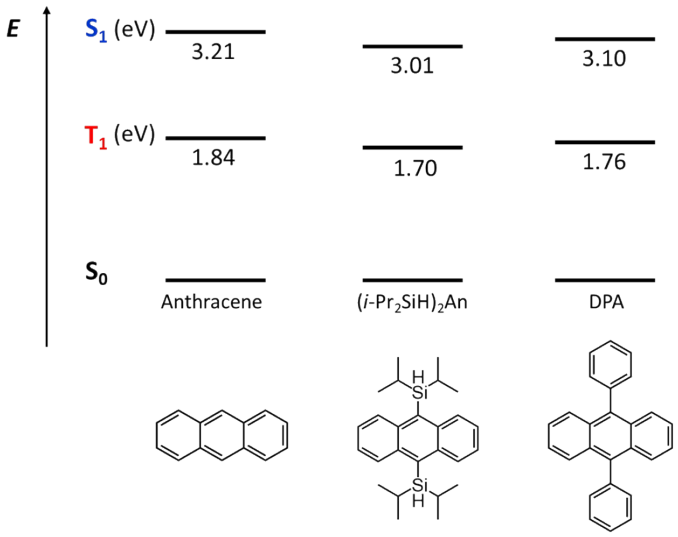

Figure S3. Energy levels of excited singlet states (S_1) and excited triplet states (T_1) of anthracene, (i-$Pr_2SiH)_2An$, and DPA calculated at TD-B3LYP/6-311++G (d,p)//B3LYP/6-311G(d,p) in the Gaussian 09 software.[3]

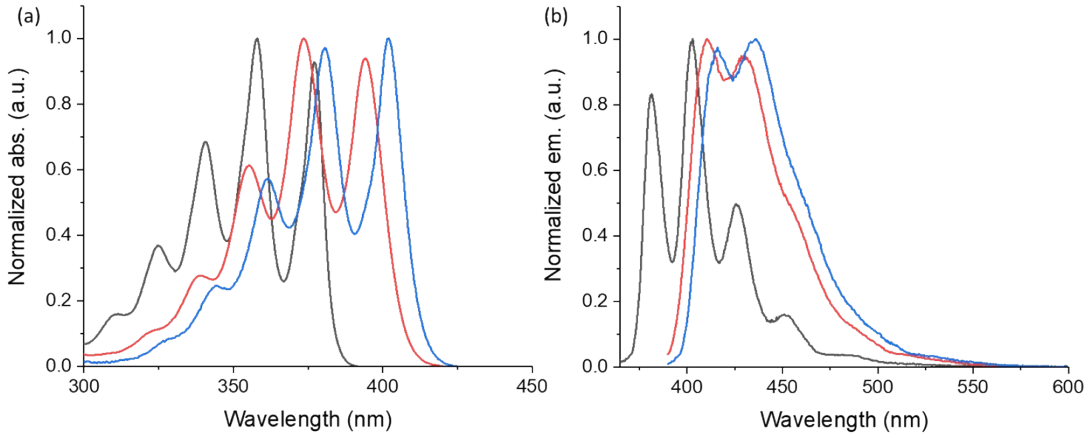

Figure S4. (a) Absorption and (b) emission spectra of anthracene (black, λ_{ex} = 350 nm), DPA (red, λ_{ex} = 380 nm) and (i-$Pr_2SiH)_2An$ (blue, λ_{ex} = 380 nm) in THF (10 μM). The 0-0 absorption peaks of anthracene, (i-$Pr_2SiH)_2An$, and DPA are located at 3.29, 3.08, and 3.15 eV, which agrees well with the DFT calculation results (Figure S3).

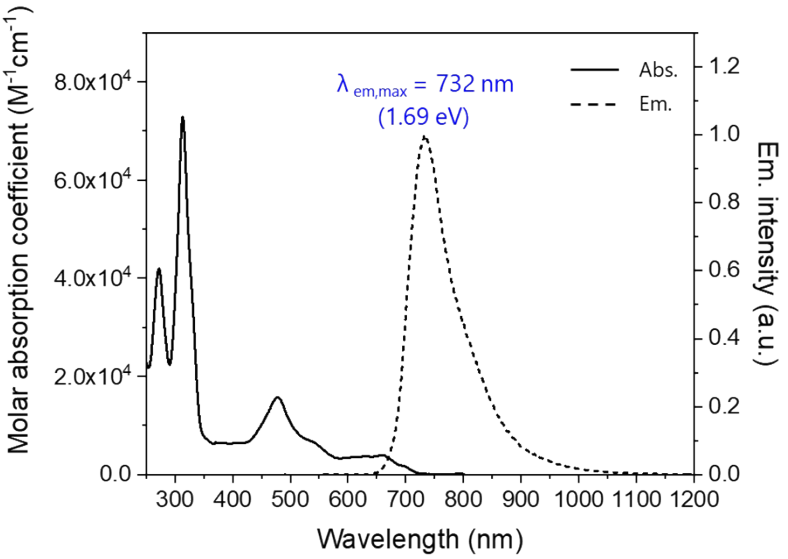

Figure S5. Absorption and emission spectra of $Os(tpy)_2^{2+}$ in deaerated DMF (20 μM, λ_{ex} = 480 nm).

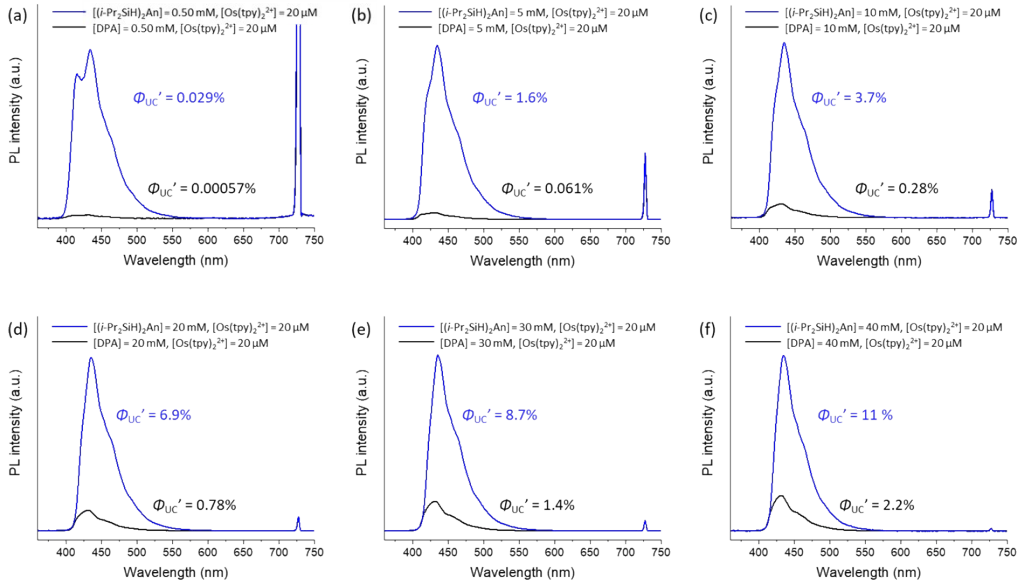

Figure S6. PL spectra and TTA-UC efficiencies of $(i\text{-}Pr_2SiH)_2An\text{-}Os(tpy)_2^{2+}$ and $DPA\text{-}Os(tpy)_2^{2+}$ in deaerated THF under the various acceptor concentration conditions (λ_{ex} = 724 nm, 610 nm short-pass filter, excitation intensity I_{ex} = 247 Wcm^{-2}). $[Os(tpy)_2^{2+}]$ = 20 μM, [Acceptor] = (a) 0.50 mM, (b) 5 mM, (c) 10 mM, (d) 20 mM, (e) 30 mM, (f) 40 mM.

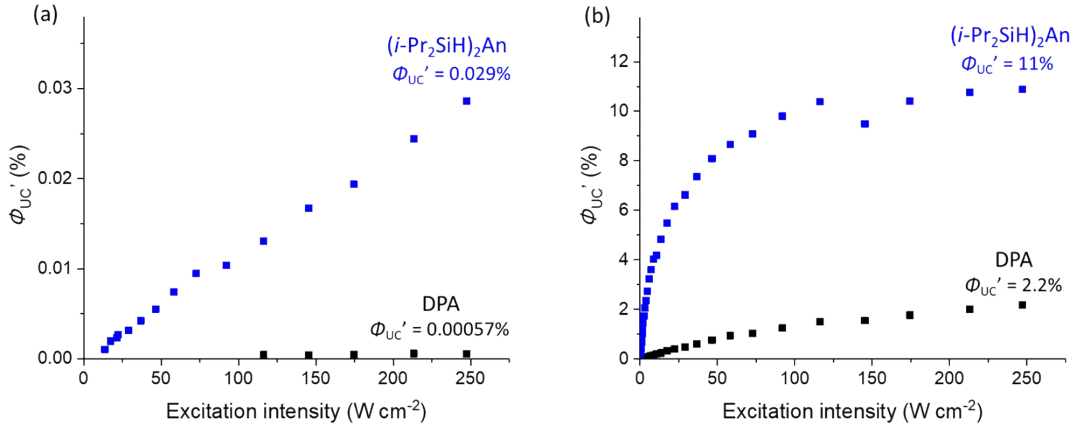

Figure S7. TTA-UC efficiencies of $(i\text{-Pr}_2\text{SiH})_2$An-$Os(tpy)_2^{2+}$ and DPA-$Os(tpy)_2^{2+}$ in deaerated THF with various excitation intensities (λ_{ex} = 724 nm). (a) [Acceptor] = 0.50 mM, $[Os(tpy)_2^{2+}]$ = 20 μM, (b) [Acceptor] = 40 mM, $[Os(tpy)_2^{2+}]$ = 20 μM.

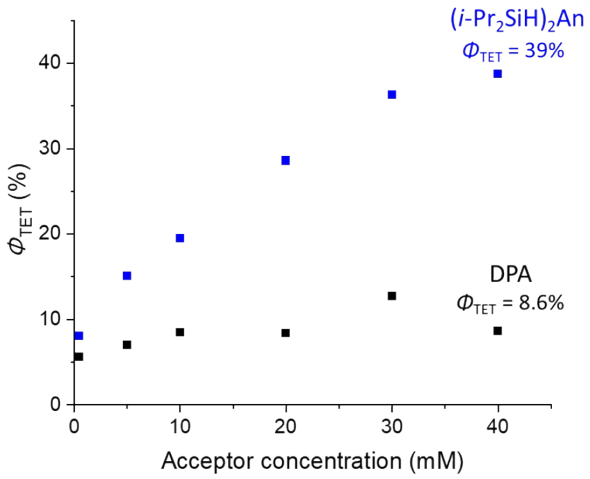

Figure S8. TET efficiencies of $(i\text{-Pr}_2\text{SiH})_2$An-$Os(tpy)_2^{2+}$ and DPA-$Os(tpy)_2^{2+}$ in deaerated THF at various acceptor concentrations (λ_{ex} = 724 nm, $[Os(tpy)_2^{2+}]$ = 20 μM).

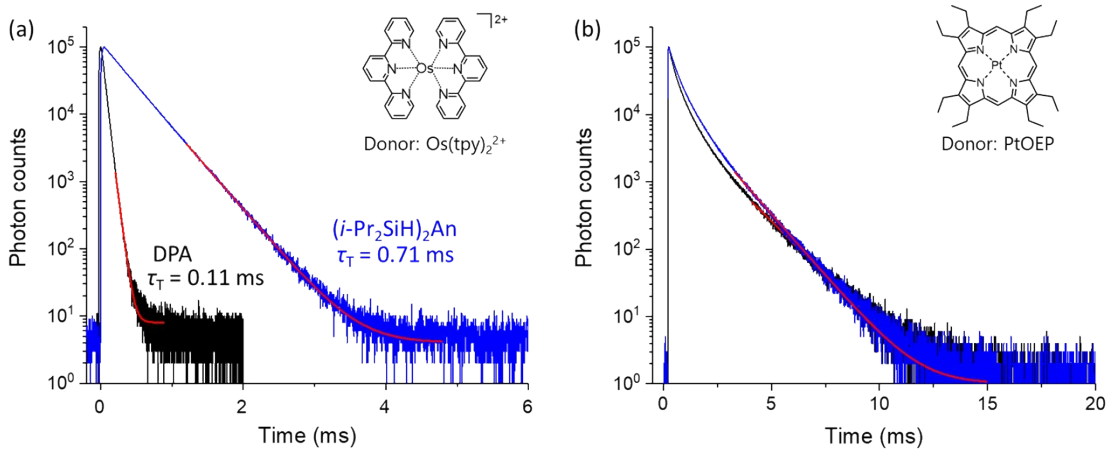

Figure S9. (a) UC emission decays of (i-Pr$_2$SiH)$_2$An (40 mM)-Os(tpy)$_2^{2+}$ (20 μM) and DPA (40 mM)-Os(tpy)$_2^{2+}$ (20 μM) at 430 nm in deaerated THF under pulsed excitation at 632 nm. (b) UC emission decays of (i-Pr$_2$SiH)$_2$An (10 mM)-PtOEP (10 μM) at 440 nm and DPA (10 mM)-PtOEP (10 μM) at 430 nm in deaerated THF under pulsed excitation at 531 nm. Red lines show the results of tail fitting of the data in the long-time ranges.

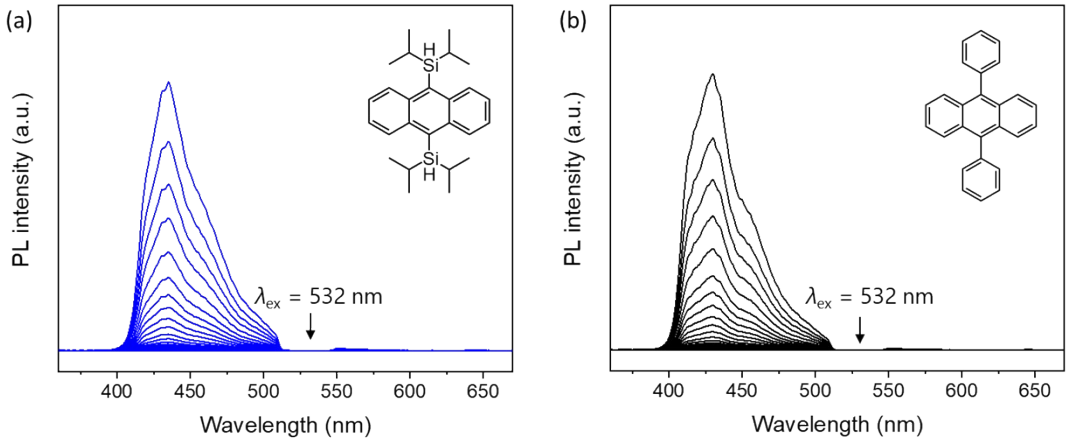

Figure S10. UC emission spectra of (a) (i-Pr$_2$SiH)$_2$An (10 mM)-PtOEP (10 μM) and (b) DPA (10 mM)-PtOEP (10 μM) in deaerated THF with various excitation intensity from 0.10 mWcm^{-2} to 3.2 Wcm^{-2} (λ_{ex} = 532 nm, 532 nm notch filter).

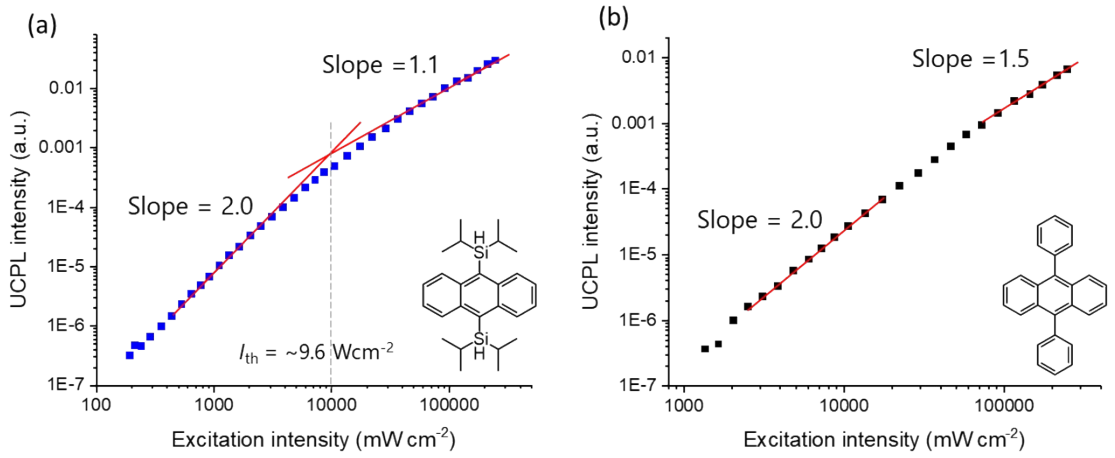

Figure S11. Excitation intensity dependence of UC emission for (a) (*i*-$Pr_2SiH)_2An$ (40 mM)-$Os(tpy)_2^{2+}$ (20 μM) and (b) DPA (40 mM)-$Os(tpy)_2^{2+}$ (20 μM) at 430 nm in deaerated THF (λ_{ex} = 724 nm). Red lines show the linear fitting results.

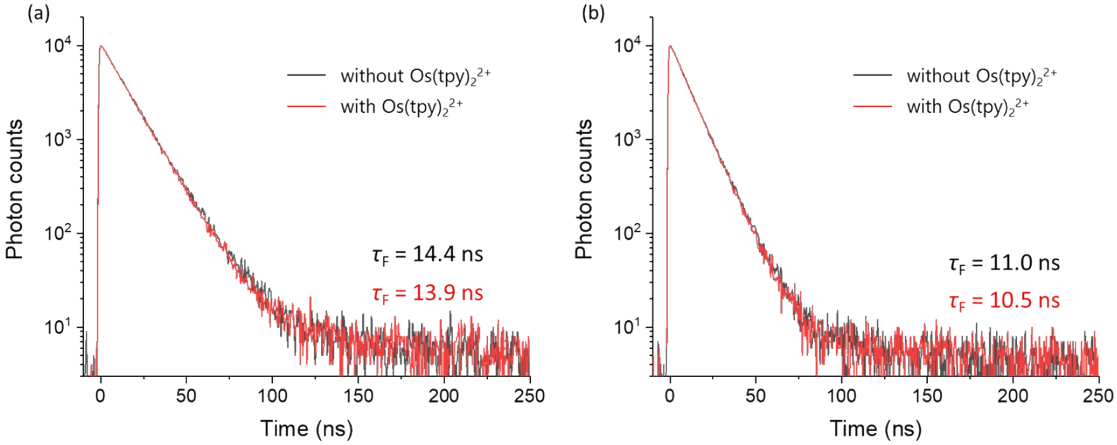

Figure S12. Fluorescence decays of (a) (*i*-$Pr_2SiH)_2An$ (40 mM) and (b) DPA (40 mM) at 440 nm with or without $Os(tpy)_2^{2+}$ (20 μM) in deaerated THF under pulsed excitation at 365 nm.

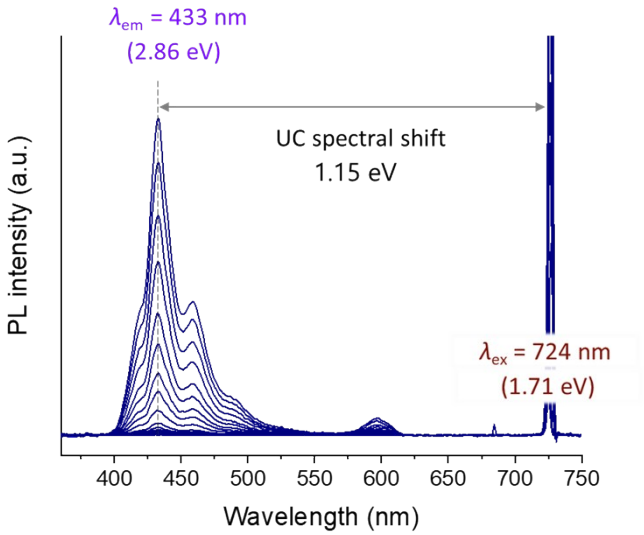

Figure S13. UC emission spectra of the solid sample of (i-$Pr_2SiH)_2$An-$Os(tpy)_2^{2+}$ ($Os(tpy)_2^{2+}$/(i-$Pr_2SiH)_2$An = 0.1 mol%) with various excitation intensity from 0.55 Wcm^{-2} to 64 Wcm^{-2} (λ_{ex} = 724 nm, 610 nm short-pass filter).

References.

1. N. Yanai, K. Suzuki, T. Ogawa, Y. Sasaki, N. Harada and N. Kimizuka, *J. Phys. Chem. A*, 2019, **123**, 10197-10203.
2. M. Montalti, A. Credi, L. Prodi and M. T. Gandolfi, *Handbook of Photochemstry,* 3rd ed., CRC Press, Boca Raton, 2006.
3. M. J. Frisch, G. W. Trucks, H. B. Schlegel, G. E. Scuseria, M. A. Robb, J. R. Cheeseman, G. Scalmani, V. Barone, B. Mennucci, G. A. Petersson, H. Nakatsuji, M. Caricato, X. Li, H. P. Hratchian, A. F. Izmaylov, J. Bloino, G. Zheng, J. L. Sonnenberg, M. Hada, M. Ehara, K. Toyota, R. Fukuda, J. Hasegawa, M. Ishida, T. Nakajima, Y. Honda, O. Kitao, H. Nakai, T. Vreven, J. A. Montgomery, Jr., J. E. Peralta, F. Ogliaro, M. Bearpark, J. J. Heyd, E. Brothers, K. N. Kudin, V. N. Staroverov, T. Keith, R. Kobayashi, J. Normand, K. Raghavachari, A. Rendell, J. C. Burant, S. S. Iyengar, J. Tomasi, M. Cossi, N. Rega, J. M. Millam, M. Klene, J. E. Knox, J. B. Cross, V. Bakken, C. Adamo, J. Jaramillo, R. Gomperts, R. E. Stratmann, O. Yazyev, A. J. Austin, R. Cammi, C. Pomelli, J. W. Ochterski, R. L. Martin, K. Morokuma, V. G. Zakrzewski, G. A. Voth, P. Salvador, J. J. Dannenberg, S. Dapprich, A. D. Daniels, O. Farkas, J. B. Foresman, J. V. Ortiz, J. Cioslowski, D. J. Fox, Gaussian 09, Revision D.01, Gaussian, Inc., Wallingford CT, 2013.
4. S. Kyushin, M. Ikarugi, M. Goto, H. Hiratsuka and H. Matsumoto, *Organometallics*, 1996, **15**, 1067-1070.
5. Y. Sasaki, M. Oshikawa, P. Bharmoria, H. Kouno, A. Hayashi-Takagi, M. Sato, I. Ajioka, N. Yanai and N. Kimizuka, *Angew. Chem. Int. Ed.*, 2019, **58**, 17827-17833.
6. R. Dennington, T. A. Keith, J. M. Millam, GaussView, version 5, Semichem Inc., Shawnee Mission, KS, 2009.